Journal of Experimental Botany, Vol. 56, No. 418, pp. 2239–2251, August 2005
doi:10.1093/jxb/eri223 Advance Access publication 4 July, 2005

Journal of Experimental Botany

RESEARCH PAPER

Cellular damage induced by cadmium and mercury in *Medicago sativa*

Cristina Ortega-Villasante[1,2], Rubén Rellán-Álvarez[1,2], Francisca F. Del Campo[1], Ramón O. Carpena-Ruiz[2] and Luis E. Hernández[1,*]

[1] *Laboratorio de Fisiología Vegetal, Departamento de Biología, Universidad Autónoma de Madrid, Campus de Cantoblanco, E-28049 Madrid, Spain*

[2] *Departamento de Química Agrícola, Universidad Autónoma de Madrid, Campus de Cantoblanco, E-28049 Madrid, Spain*

Received 10 March 2005; Accepted 10 May 2005

Abstract

Alfalfa (*Medicago sativa*) plantlets were exposed to Cd or Hg to study the kinetics of diverse stress indexes. In the so-called beaker-size hydroponic system, plantlets were grown in 30 μM of Cd or Hg for 7 d. Oxidative stress took place and increased over time, a linear response being observed with Cd but not with Hg. To improve the sensitivity of the stress assays used, a micro-assay system, in which seedlings were exposed for 24 h, was developed. Phytotoxicity of metals, quantified as growth inhibition, was observed well before there was any change in the non-protein thiol tissue concentration. When measured with conventional techniques, oxidative stress indexes did not show significant variation. To trace early and small plant responses to Cd and Hg, a microscopic analysis with novel fluorescent dyes, which had not yet been exploited to any significant extent for use in plants, was conducted. These fluorescent probes, which allowed minute cellular responses to 0, 3, 10, and 30 μM of both metals to be visualized in the roots of the alfalfa seedlings, were: (i) 2′,7′-dichlorofluorescin diacetate that labels peroxides; (ii) monochlorobimane that stains reduced glutathione/homoglutathione (GSH/hGSH); and (iii) propidium iodide that marks nuclei of dead cells. Oxidative stress and cell death increased after exposure for 6–24 h to Cd and Hg, but labelling of GSH/hGSH decreased acutely. This diminution might be the result of direct interaction of GSH/hGSH with both Cd and Hg, as inferred from an *in vitro* conjugation assay. Therefore, both Cd and Hg not only compromised severely the cellular redox homeostasis, but also caused cell necrosis. In plants treated with 1 mM L-buthionine sulphoximine, a potent inhibitor of GSH/hGSH synthesis, only the oxidative stress symptoms appeared, indicating that the depletion of the GSH/hGSH pool was not sufficient to promote cell death, and that other phytotoxic mechanisms might be involved.

Key words: Alfalfa, Cd, cell damage, fluorescence, GSH/hGSH, H_2DCFDA, Hg, MCB, microscopy, oxidative stress.

Introduction

Due to diverse human activities, such as mining and smelting, metal pollution is becoming a major risk to many ecosystems. Among the pollution-producing metals, cadmium (Cd) and mercury (Hg) are regarded as non-essential elements, with no known physiological functions. They are extremely toxic to plants and animals, have a long half-life and are extremely persistent in the environment (Salt *et al*., 1995). Exposure of plants even to minute concentrations may lead to the alteration of many cellular processes and structures (Hall, 2000). One of the characteristic effects of metal poisoning, observable at an early stage, is a reduction in cell proliferation and growth (Schützendübel *et al*., 2001). It has also been associated with the appearance of oxidative stress (Schützendübel and Polle, 2002). Accumulation of reactive oxygen species (ROS), leading to an oxidative burst, is thought to increase cellular damage through oxidation of several macro-molecules (Hall,

* To whom correspondence should be addressed. Fax: +34 91 4978344. E-mail: luise.hernandez@uam.es

Abbreviations: BSO, L-buthionine sulphoximine; Cys, cysteine; GSH, glutathione; DIC, differential interference contrast; GSSG, oxidized glutathione; GST, glutathione *S*-transferase; H_2DCFDA, 2′,7′-dichlorofluorescin diacetate; hGSH, homoglutathione; MCB, monochlorobimane; N-AcCys, *N*-acetyl cysteine; PCs, phytochelatins; PI, propidium iodide; ROS, reactive oxygen species.

2000), such as lipids (Sandalio *et al*., 2001) and proteins (Romero-Puertas *et al*., 2002). Some metals such as Fe^{2+} and Cu^{+} might induce oxidative cell damage coupled to their auto-oxidation, through Fenton-type reactions. However, this type of reaction has not been described for either Cd^{2+} or Hg^{2+} in plants (Schützendübel and Polle, 2002), despite the evidence of oxidative stress induction in different plants after exposure to Cd (Lozano-Rodríguez *et al*., 1997; Dixit *et al*., 2001; Schützendübel *et al*., 2002) and to Hg (Cho and Park, 2000). Therefore, plant redox homeostasis might be compromised by the uptake of Cd and Hg.

Other cellular responses observed after addition of heavy metals are changes in thiol-peptide metabolism (Rauser, 1991). Hence, accumulation of phytochelatins (PCs) might play a central role in metal detoxification (Cobbett and Goldsbrough, 2002). Phytochelatins are synthesized by phytochelatin synthase from reduced glutathione (GSH), the major non-protein thiol in plants, and key for many functions in plant metabolism. Several plants accumulate homologous non-protein thiols with changes in their constituent amino acids; for example, in legumes the glycine of GSH is substituted by alanine, producing homoglutathione (hGSH; Matamoros *et al*., 1999). The balance between the reduced and the oxidized form of glutathione (GSSG) is crucial for the enzymatic systems that scavenge ROS (Noctor *et al*., 2002). A common response to heavy metals is depletion of GSH, and a subsequent raise of GSSG (Rauser, 1995; Xiang and Oliver, 1998). Moreover, some authors link the drainage of GSH, caused by the synthesis of PCs, to the impairment of the cellular redox status (Meuwly and Rauser, 1992; Noctor *et al*., 1998; Xiang and Olivier, 1998). Taken together, these previous reports suggest that maintenance of the GSH pool is important for plant tolerance to metals.

To study oxidative stress in response to heavy metals, a plethora of experiments have been carried out, using different plant species, doses of metals, and exposure times, as reviewed by Schützendübel and Polle (2002). In most of the studies, oxidative stress symptoms appeared when treatments were long enough to attain substantial metabolic changes. In such experiments, the effects caused by relatively long exposure to metal might reflect a general failure of the plant metabolism. Little is known about the early stages. Even though toxic metals can clearly induce oxidative stress, the mechanisms underlying this cellular response remain to be elucidated. The development of new microscopy techniques and the increased availability of more sensitive and specific fluorescent probes makes it possible to trace minute changes of various physiological parameters at cell level *in vivo* (Fricker and Meyer, 2001). Thus, using monochlorobimane (MCB), cellular GSH content was analysed recently in several plant tissues (Sánchez-Fernández *et al*., 1997; Hartmann *et al*., 2003), some of them subjected previously to salt stress (Gutiérrez-Alcalá *et al*., 2000). In addition, cellular ROS accumulation at several developmental stages under induced oxidative stress has been followed by the oxidation of 2′,7′-dichlorofluorescin diacetate (H_2DCFDA) to fluorescent derivatives, i.e. 5- (and-6)-carboxy-2′,7′-dichlorofluorescein (Allan and Fluhr, 1997; Potikha *et al*., 1999; Bethke and Jones, 2001). The referred novel fluorescent dyes, which have not yet been exploited to any significant extent in plants, might help in understanding the processes, which occur in cells exposed to toxic metals, by allowing them to be followed in a more precise way. Here it is reported how these fluorescent probes and fluorescence microscopy were used to study early stress symptoms in root epidermal cells of alfalfa (*Medicago sativa*) exposed to Cd and Hg for 6 h and 24 h. It was possible to visualize minute damage caused by both metals, as observed by increased oxidative stress, higher level of cell death, and depletion of the GSH/hGSH pool.

Materials and methods

Chemicals

Stocks of 100 mM MCB and H_2DCFDA in DMSO were stored at –20 °C in 10 μl aliquots. Aliquots were thawed and diluted immediately prior to use. Propidium iodide (PI) was prepared as a 1 mg ml^{-1} stock solution in deionized water and used at a final concentration of 25 μM. All dyes were purchased from Molecular Probes. A stock solution of 100 mM L-buthionine sulphoximine (BSO; Sigma) was prepared in deionized water, and stored at −20 °C. $3(CdSO_4).8H_2O$ and $HgCl_2$ were analytical grade purchased from Merck.

Plant material

Seeds of *Medicago sativa* var. Aragon were surface-sterilized for 5 min in 5% (v/v) commercial bleach. After rinsing several times with sterile water, seeds were soaked overnight at 4 °C and allowed to germinate on 1.5% (w/v) agar (Pronadisa), in square Petri dishes (10×10 cm), in complete darkness for 24 h at 28 °C. Homogenous seedlings were chosen and carefully transferred to the beaker-size and micro-assay hydroponic systems.

Beaker-size hydroponic system

Preliminary analyses of metal-induced stress were performed in the so-called beaker-size hydroponic system. Selected seedlings were placed in plastic grid holders, suspended in glass cylinders containing 150 ml of Murashige–Skoog nutrient solution at pH 6.0 (Duchefa Biochemie). Continuous aeration was provided, and plants grew for 12 d under controlled environment conditions (16 h light photoperiod at an average photon flux of 150 μmol m^{-2} s^{-1}, at 25 °C day/18 °C night). Heavy metals were then supplied at a high concentration (30 μM) to ensure quick plant responses, and samples were taken at different intervals from the beginning of the metal treatments.

Micro-assay system

Selected seedlings were transferred to the so-called Fåhraeus slides culture system (Heidstra *et al*., 1994). Seedlings were carefully placed in a frame like a sandwich, which was hand-made by sticking a coverslip over a microscope slide with several drops of silicone adhesive/sealant. The frames were kept in Schieferdecker glass staining containers, filled with sterilized Murashige–Skoog nutrient solution at pH 6.0, and kept under the same controlled environmental conditions described above. This system provided a suitable medium for plant growth, where seedlings acclimatized for 24 h prior to

treatment with Cd or Hg, at 0, 3, 10, and 30 μM final concentration, or with 1 mM BSO as indicated. Then, plants were allowed to grow for a further 24 h.

Growth measurements

Roots from the beaker-size experiment and seedlings from the microscopic system were sampled at regular intervals (8–10 plants), and maximum root or seedling length was measured. Growth was expressed relative to control plants, and data given were the average of at least three independent experiments ±standard deviation, calculated according to the following expression, in which HM is the heavy metal treatment and C is the control:

$$\text{Relative growth inhibition } (\%) = [(\text{root/seedling length}_{C} - \text{root/seedling length}_{HM})/\text{root/seedling length}_{C}] \times 100$$

Oxidative stress indexes

Lipid peroxidation: Lipid peroxidation was estimated *in vitro* after the formation of malondialdehyde, a by-product of lipid peroxidation that reacts with thiobarbituric acid. The resulting chromophore absorbs at 535 nm, and the concentration was calculated directly from the extinction coefficient of 1.56×10^{5} M cm^{-1}. Ground frozen tissue (0.1–0.2 g) was transferred to a screw-capped 1.5 ml Eppendorf tube, and homogenized following addition of 1 ml of TCA–TBA–HCl reagent [15% (w/v) trichloroacetic acid (TCA), 0.37% (w/v) 2-thiobarbituric acid (TBA), 0.25 M HCl, and 0.01% butylated hydroxytoluene]. After homogenization, samples were incubated at 90 °C for 30 min in a hot block, then chilled in ice, and centrifuged at 12 000 *g* for 10 min. Absorbance was measured at 535 nm and 600 nm, the last one to correct the non-specific turbidity.

Protein oxidation: Proteins were extracted from 0.5 g ground frozen tissue with 0.5 ml of extraction buffer [0.1 M Na-phosphate buffer, 0.2% Triton X-100 (v/v), 1 mM EDTA, and 1 mM PMSF at pH 7.4]. After centrifugation at 12 000 *g* for 15 min, protein concentration was determined in the supernatant using the Protein Assay reagent (BioRad), with thyroglobulin as standard. Protein oxidation was measured as carbonyl concentration, following the protocol described by Romero-Puertas *et al*. (2002), with minor modifications. After incubation with 10 mM dinitrophenylhydrazine, proteins were precipitated with 20% TCA. To facilitate pellet re-dissolution, excess acid was washed with 10% H_2O in ethanol:ethyl acetate (1:1, v/v). The pellet was disrupted using an Eppendorf potter, and then incubated at 40 °C for 30 min. After incubation, the suspension was centrifuged at 12 000 *g* for 5 min, and absorbance was measured at 370 nm (carbonyl concentration) and at 280 nm (total protein concentration).

Analysis of non-protein thiols by HPLC

HPLC (high performance liquid chromatography) was used to quantify non-protein thiols in acidic extracts. Plant tissue was ground in liquid N_2, and 0.1 g of frozen powder was thoroughly mixed with 300 μl of 0.25 N HCl. To quantify them, a spike of *N*-acetyl cysteine (N-AcCys) was added as internal standard prior to homogenization (Howden *et al*., 1995) at a final concentration of 50 μM. The homogenate was centrifuged twice for 15 min at 12 000 *g* and at 4 °C in Eppendorf tubes. The clear supernatant was transferred to a boron–silica glass injection vial. The separation and detection protocol used was that of Meuwly *et al*. (1995) with minor changes. One hundred and twenty-five microlitres was injected in a PLRPS C18 column (250×4.6 mm; Polymer Laboratories) coupled to a Kromasil-C18 precolumn (30×4.6 mm; Scharlab), and eluted with a gradient of solvent A [98:2 H_2O:acetonitrile (v/v) plus 0.01% TFA] and solvent B (2:98 H_2O:acetonitrile (v/v) plus 0.01% TFA). The gradient programme, as for % solvent B, was: 2 min, 0%; 25 min, 25%; 26 min, 50%; 30 min, 50%; 35 min, 0%, 45 min, 0%. The chromatography was performed in the Alliance 2695 HPLC system (Waters). Detection was achieved after post-column derivatization with Ellman's reagent [1.8 mM DTNB (5,5-dithio-bis(2-nitrobenzoic) acid) in 300 mM K-phosphate, 15 mM EDTA at pH 7.0]. The reaction took place in a thermostatted 1.8 ml reactor at 37 °C, as described by Rauser (1991). The derivative compound, 5-mercapto-2-nitrobenzoate, had an absorption maximum at 412 nm.

Dye loading and fluorescence microscopy

Confocal laser scanning microscopy: A TCS SP2 confocal microscope (Leica) was used to visualize GSH levels in intact roots after *in vivo* conjugation with MCB in a reaction catalysed by GST enzyme, yielding a GSH–MCB conjugate (Fricker and Meyer, 2001; Meyer *et al*., 2001). Labelling was carried out for 15–20 min with a solution containing 1 ml of 25 μM MCB and 5 mM sodium azide, keeping the seedlings all the time in the micro-assay system frames. Azide was used to deplete ATP levels, and thereby to avoid ATP-dependent vacuolar sequestration of fluorescent conjugate, which could undergo quenching of the fluorescence signal. To monitor cell death, PI was added as a counter-stain to a final concentration of 25 μM. PI marks the condensed nuclei of dead cells when it permeates damaged plasmalemma, and also labels the whole cell walls. The fluorescent GSH–MCB conjugate was excited with an argon-UV laser (351–364 nm) and the emission monitored at 477 nm. In a second channel, a helium–neon laser (543 nm) excited PI, its emission being recorded at 620 nm. Microscopy images shown represent observations of at least 10 independent experiments.

Epifluorescence microscopy: The cellular peroxidation level was studied after labelling for 10–15 min with a 10 μM H_2DCFDA solution, and PI was also added as a counter-stain to a final concentration of 25 μM. Samples were observed by epifluorescence microscopy with a BX61 microscope equipped with a U-M51004V2 cube and coupled to a DP70 CCD camera (Olympus). Segments subjected to morphological analysis corresponded to root hairs nearly finishing elongation, when most of the hair tip is vacuolized.

Quantification of fluorescence staining

Confocal laser scanning microscopy: GSH–MCB adduct formation and PI labelling were quantified as average pixel density of each fluorescence channel, in defined regions of interest, with Leica confocal software. The data, taken from at least five independent snapshots from different roots, were corrected against the background signal according to the manufacturer instructions.

Epifluorescence microscopy: Cell peroxidation and death were subjected to manual morphological analysis, annotating the number of cells showing green fluorescence of oxidized H_2DCFDA and condensed nuclei labelled with PI. Data were expressed as a percentage of the total number of cells visualized in the field under analysis.

In vitro *GSH–MCB conjugation and GST activity*

Several assays were performed in a fluorescence plate reader to test *in vitro* conjugation of GSH with MCB, and to quantify the extent of fluorescence quenching caused by Cd and Hg. Glutathione *S*-transferase (GST) enzyme (0.2 U; Sigma), prepared from a stock solution (0.2 U μl^{-1} in 25 mM TRIS–HCl buffered at pH 7.0, diluted prior to use in 30 μl of reaction buffer made of PIPES 200 mM, at pH 6.5), was added to each well of a 96-well microtitre plate (flat dark bottom; Bibby Sterilin) previously filled with 110 μl of miliRO H_2O. Subsequently, 10 μl of different stock solutions of GSH were added to obtain final concentrations of 0.1, 0.2, and 0.4 mM. Heavy metals were supplied to reach final concentrations from 0.05 to 0.4 mM, by transferring 25 μl of the appropriate stocks of Cd or Hg. After

incubation for 30 min, the reaction was triggered by adding 25 µl MCB (final concentration of 25 µM). Fluorescence was measured in a fluorescence plate reader (Spectrafluor; TECAN) at 485 nm, after excitation at 400 nm.

Endogenous GST activity of *M. sativa* seedlings was determined *in vitro* using a similar experimental procedure to that described above. Extracts were prepared from N_2 (l) frozen tissues: 0.1 g of frozen ground material was homogenized in extraction buffer at a 1:2 (w/v) ratio [25 mM TRIS–HCl at pH 7.8, 1 mM dithiothreitol; supplemented with 1 mM phenylmethylsulphonylfluoride and protease Ccocktail inhibitor (P2714; Sigma)], in the presence of 1% polyvinylpolypyrrolidone (w/w), using a chilled mortar, keeping material at 4 °C in all subsequent steps. The homogenate was clarified by centrifuging for 15 min at 16 500 *g*. The protein concentration in the resulting extract was determined using the protein assay reagent (BioRad), with thyroglobulin as standard. Ten milligrams of protein were added per well of a 96-well microtitre plate, containing the same components as described above (except metals), and the reaction was also triggered by adding 25 µl of MCB to a final concentration of 25 µM. GST activity in plant extracts (µmol GSH–MCB min^{-1} mg^{-1} protein) was calculated in the linear range of the assay, using 0.02 µmol min^{-1} mg^{-1} of commercial GST activity as standard (Sigma).

Statistical analysis

Data are given as means ±standard deviation of at least three independent experiments. The mean differences were compared utilizing Duncan's multiple range test with SPSS for Windows (Release 12.0; SPSS Inc.)

Results

Ca- and Hg-dependent growth inhibition and oxidative damage

High concentrations of both metals, well over the levels found in polluted areas (30 µM), were used to find the earliest deleterious effects in *M. sativa* plants. In the beaker-size hydroponic system, both metals clearly produced a severe reduction in plant root length. Cd caused a continuous growth inhibition, reaching values around 30% after 7 d of treatment (Fig. 1A). However, Hg-treated plants suffered an abrupt inhibition (30–40%) within the first 24 h of exposure, an effect that remained almost constant until the end of the experiment (Fig. 1A). Lipid peroxidation in shoots and roots from plants exposed to Cd also increased continuously, and reached maximum levels after 7 d (Fig. 1B, C). Hg caused a sudden increment of lipid peroxidation in both shoot and root before 24 h, and the peroxidation level remained stable at the different times analysed (Fig. 1B, C). Another oxidative stress parameter assessed was protein oxidation, which obtained a very similar pattern to lipid peroxidation. There was a persistent increase for Cd, with the highest levels after 7 d of treatment, and a sharp rise with Hg within the first 24 h that continued steadily through the experimental time (data not shown).

To evaluate how genuine the observed stress indexes caused by metals through the time were, a regression analysis was carried out. Thus, Person's coefficient (0.92–0.98) revealed that responses of Cd-treated plants

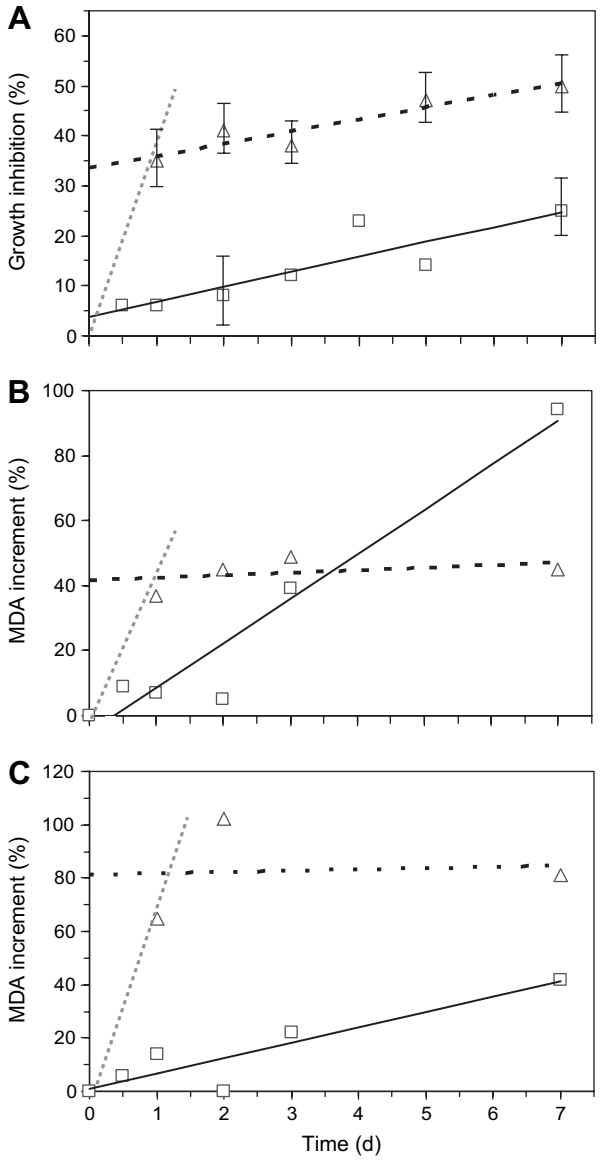

Fig. 1. Stress indexes of *M. sativa* plants grown in the beaker-size hydroponic system and exposed to 30 µM Cd (squares, continuous line) or 30 µM Hg (triangles, dashed line), measured at several intervals. The estimated linear phase is represented by a doted line. All values are relative to control data (%). (A) Growth inhibition of roots; (B) lipid peroxidation of shoot; (C) lipid peroxidation of root; both measured as malondialdehyde equivalents and calculated relative to control data.

adjusted clearly to a line (Fig. 1). However, plants exposed to Hg showed lower Pearson's coefficients for growth inhibition (0.73) and increased malondialdehyde (below 0.50 in shoots and roots). These data do not adjust well to a line; once a high first value is reached, it remains in a steady state, indicating that Hg caused both a stronger and an earlier damage than Cd.

It appears that in Hg-treated plants the early linear range in the plant response could have been missed, as it might have taken place within the first 24 h (Fig. 1). To test this hypothesis, the sampling period was shortened by

using the micro-assay system, which consequently permitted the analysis of early metal effects. The same stress indexes as in the beaker-size system experiments were analysed, but only growth inhibition reflected a toxicity response to Cd and Hg (Fig. 2). Both metals caused inhibition of seedling growth within 24 h, following a steady linear increase from the beginning of the treatment. In this case, Pearson's coefficient values were 0.95 and 0.93 for Hg- and Cd-treated plants, respectively. Moreover, Hg showed stronger toxic effects, as growth inhibition reached 40% after 24 h, while Cd only attained about 30% (Fig. 2).

Paradoxically, the oxidative stress indexes that responded clearly to Cd and Hg exposure in the beaker-size system did not reflect a consistent response to both metals during the sampling period of the micro-assay (data not shown). However, growth was affected at the very beginning of the treatments (Fig. 2), in agreement with the effects observed in Scots pine and poplar seedling roots briefly exposed to Cd (Schützendübel *et al*., 2001, 2002).

Analysis of non-protein thiols by HPLC

To explore a way of following early stress responses, the variation in non-protein thiol composition (Cobbett and Goldsbrough, 2002) was analysed. First, the main thiols were identified in whole seedling extracts from plants exposed to Cd or Hg in the microscopic assay (Fig. 3), identification being achieved by co-injections with commercially available standards. The major non-protein thiol found corresponded to hGSH. Its concentration was around 300 nmol g^{-1} FW (Table 1), a value that agrees with that found in alfalfa by other authors (Matamoros *et al*., 1999). The other identified peaks corresponded to cysteine (Cys) and GSH, together accounting for <50% of the observed hGSH concentration (Table 1).

New peaks, which corresponded to putative PCs, appeared at longer times of elution in extracts from seedlings treated with Cd after 24 h (Fig. 3B). This identification was based on: (i) similar retention times observed for PCs by Rauser, Meuwly, and co-workers using similar chromatographic conditions (Rauser, 1991; Meuwly *et al*., 1995); and (ii) the fact that the size of those peaks increased concomitantly with prolonged exposure to Cd (data not shown), a typical response of PC accumulation (Cobbett and Goldsbrough, 2002). On the other hand, Hg exposure had a milder effect on the accumulation of PCs, since only traces were observed (Fig. 3C; Table 1). Similar results were found in extracts from plants grown in the beaker-size system; at longer exposure times, larger amounts of putative PCs were found in Cd-treated plants than in those supplied with Hg (data not shown). In addition, integration of non-protein thiol peaks after 24 h of treatment revealed a remarkable decrease of hGSH levels in Hg-treatments while, in those exposed to Cd, the hGSH content was similar to the control (Table 1). Even though differences in

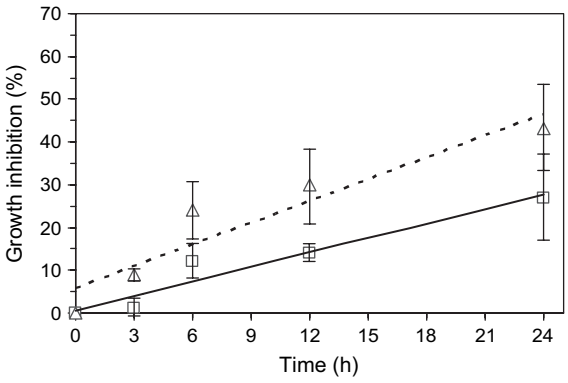

Fig. 2. Growth inhibition of *M. sativa* seedlings sampled at several times and exposed to 30 μM Cd (squares) or Hg (triangles) in the micro-assay hydroponic system.

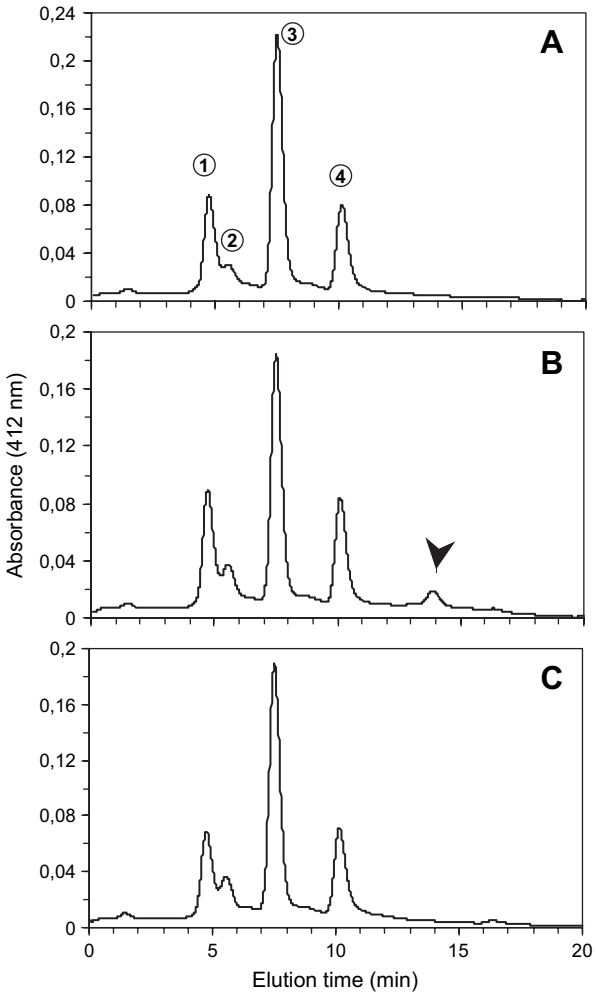

Fig. 3. HPLC elution profile of non-protein thiols extracted from *M. sativa* seedlings grown with 30 μM Cd or 30 μM Hg for 24 h after post-column derivatization with Ellman's reagent: (A) control, (B) Cd; (C) Hg. Peaks were identified using commercially available standards: 1, Cys; 2, GSH; 3, hGSH; 4, spiked internal standard of N-AcCys. In the samples of Cd-treated seedlings a new peak appeared (arrowhead), tentatively identified as phytochelatins.

Table 1. *Non-protein thiols content (nmol g^{-1} FW) in* Medicago sativa *seedlings exposed to 30 μM Cd or Hg, after several time intervals*

Concentration of each thiol peptide was calculated equivalent to the internal standard of N-AcCys. Results are the mean of at least three independent assays. Different superscript letters denote significant differences between treatments at $P < 0.05$.

Thiol	0 h	Control		Cd		Hg	
		6 h	24 h	6 h	24 h	6 h	24 h
Cys	$199.0^{c} \pm 15.8$	$109.8^{a} \pm 27.0$	$143.0^{b} \pm 1.0$	$110.3^{a} \pm 10.7$	$149.4^{b} \pm 7.8$	$111.0^{a} \pm 2.2$	$120.2^{a} \pm 21.1$
GSH	$97.4^{a} \pm 11.0$	$60.6^{b} \pm 10.6$	$63.4^{b} \pm 12.1$	$67.8^{b} \pm 8.6$	$71.0^{b} \pm 16.9$	$68.6^{b} \pm 14.4$	$80.1^{ab} \pm 14.5$
hGSH	$321.6^{a} \pm 15.0$	$309.4^{a} \pm 6.7$	$346.8^{a} \pm 51.3$	$345.1^{a} \pm 26.2$	$320.8^{a} \pm 13.3$	$336.2^{a} \pm 9.5$	$288.5^{b} \pm 17.5$
PCs	nd[a]	nd	nd	nd	48.7 ± 5.6	nd	<10.0

[a] nd, Not detected.

thiol content were detected due to the exposure of seedlings to both metals in the micro-assay system, changes were still subtle compared with the extremely toxic effect found as growth inhibition (Fig. 2).

Confocal laser scanning microscopy of thiols

None of the parameters assessed using conventional techniques reflected clearly the toxic effect of Cd and Hg found as growth inhibition. Therefore, it was necessary to use novel methods to visualize early plant responses to metal toxicity. Recently, several authors described new microscopy techniques to visualize GSH *in vivo*, based on staining it with MCB in a reaction catalysed by GST (Gutierrez-Alcalá *et al*., 2000; Hartmann *et al*., 2003). Since GST recognizes equally GSH and hGSH to detoxify several xenobiotics in *M. sativa* (Skipsey *et al*., 1997), and since MCB was used for the histochemical staining of hGSH in cowpea nodules (Dalton *et al*., 1998), it was thought that by adding MCB it would be possible to observe GSH/hGSH *in vivo.* As shown in blue pseudo-colour (Fig. 4A), GSH/hGSH–MCB staining was observed in root epidermal cells of alfalfa grown in control nutrient solution. To be sure that this fluorescence was due to the binding of MCB to GSH and hGSH, 1 mM BSO was added as a negative control. This compound, a potent inhibitor of GSH synthesis, repressed the accumulation of hGSH up to 50%, as analysed by HPLC (data not shown). BSO had a drastic effect on MCB fluorescence (Fig. 4B); root epidermal cells showed lower level of blue pseudo-colour than seedlings grown in its absence. Moreover, red fluorescence of PI was restricted to the cell walls, showing very few condensed nuclei, similar to what was observed in control seedlings (Fig. 4A).

Exposure of seedlings to 30 μM Cd or Hg for 24 h produced a remarkable decrease in GSH/hGSH–MCB staining (Fig. 4C, D). Quantification of pixel density after 6 h of treatment with 0, 3, 10, and 30 μM Cd or Hg revealed that both metals also caused a GSH/hGSH–MCB fluorescence quenching, although to a lower degree than after exposure for 24 h (Fig. 4E). Fluorescence levels were not significantly different from BSO-exposed seedlings or between different metal treatments.

Counter-staining with PI showed that cells suffered necrosis upon exposure to Cd and Hg, with characteristic condensed chromatin in the nuclei (Fig. 4C, D). The ratio of PI was calculated against GSH/hGSH–MCB labelling (the IP:MCB ratio) to estimate the degree of dead cells relative to the depletion of GSH/hGSH after 6 h and 24 h of treatment (Fig. 4E). The highest values in the IP:MCB ratio were observed in seedlings exposed to 30 μM Hg for 24 h, a treatment that led to numerous condensed nuclei and very weak GSH/hGSH–MCB staining. This effect was less pronounced in seedlings subjected to a shorter treatment interval. On the other hand, seedlings grown in 1 mM BSO for 24 h exhibited the lowest IP:MCB ratio in spite of very low staining of GSH/hGSH–MCB. This might reflect that fewer cells died than in plants grown in the presence of Cd or Hg. The differences in the IP:MCB ratio were not so evident after 6 h between seedlings treated with 1 mM BSO and the metals given.

In vitro *GSH–MCB conjugation assay*

The fluorescence quenching of MCB *in vivo* caused by Cd and Hg might have been due to: (i) depletion of GSH/hGSH cellular content; (ii) blockage of the nucleophilic SH-reacting group with the metal, which would limit the formation of the GSH/hGSH–MCB adduct; or (iii) inhibition of endogenous GST, an enzyme involved in the *in vivo* conjugation of GSH/hGSH with MCB. There is evidence that Cd and Hg have the ability to form thiolate conjugates with several non-protein thiols (Mehra *et al*., 1996; Morelli *et al*., 2002). To assess this possibility, the effects of various metal concentrations on the fluorescence produced by different GSH concentrations were compared (Fig. 5). Prior to MCB addition, GSH was allowed to interact with the metal for 30 min. At increasing concentrations of both metals there was a sharp depletion of fluorescence (Fig. 5). The quenching was stronger with Hg, fluorescence reaching nearly basal levels at 0.05 mM (Fig. 5B). Interestingly, addition of Cd caused a milder quenching; fluorescence was above the basal levels at 0.1 mM and declined completely at concentrations higher than 0.2 mM (Fig. 5A).

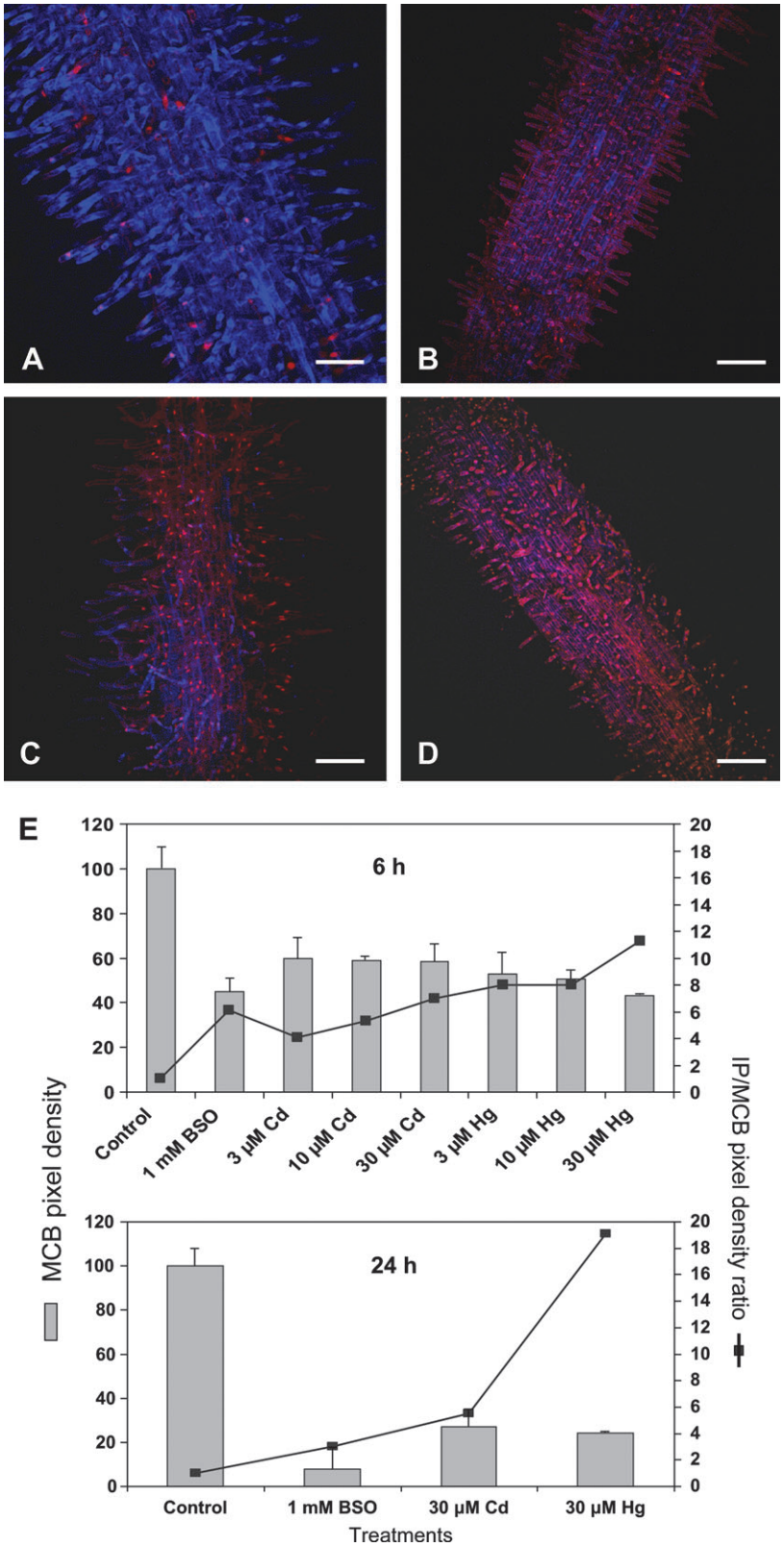

Fig. 4. Confocal imaging of *M. sativa* root cells stained with MCB that labels GSH/hGSH to give a green fluorescent adduct, after 24 h incubation with the specified chemicals: (A) control cells; (B) cells treated with 1 mM BSO; (C) 30 µM Cd; (D) 30 µM Hg. Red fluorescence corresponding to PI staining labelling cell walls and nuclei of dead cells. (E) Graph representing measurement of mean pixel density of MCB and the IP:MCB pixel density ratio of seedlings exposed for 6 h and 24 h.

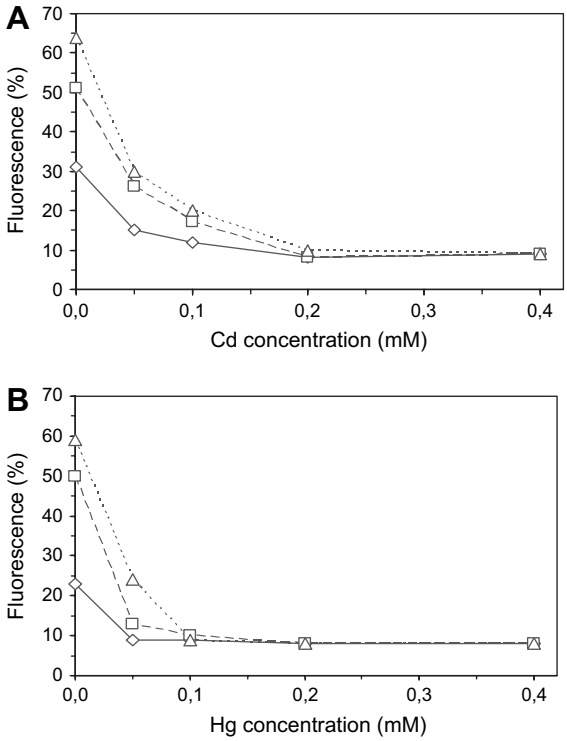

Fig. 5. *In vitro* assays to determine fluorescence quenching of the GSH–MCB adduct formed by GST at increasing concentrations of Cd (A) and Hg (B), with three different GSH concentrations: 0.1 mM (diamonds), 0.2 mM (squares), and 0.4 mM (triangles) (n=6). Data from different experiments were normalized against the fluorescence by using 1 mM GSH in the absence of metals. The standard deviation was smaller than the symbols used.

To rule out the possibility that fluorescent quenching could be due to the inhibition of GST caused by the metals, endogenous activity of *M. sativa* seedlings was determined. GST *in vitro* activity of extracts from seedlings exposed to 0, 3, 10, and 30 μM Cd or Hg was in the range of 0.94–1.05 μmol min^{-1} mg^{-1} protein. No significant differences (P <0.05) were found between treatments.

Epifluorescence microscopy of oxidative stress symptoms

Cell peroxides can be detected *in vivo* with a fluorescence microscope by the oxidation of the fluorogenic substrate H_2DCFDA (Bethke and Jones, 2001). Using this fluorescent probe, root seedlings were analysed after 24 h treatment with 30 μM Cd or Hg. In addition, roots were counterstained with PI to evaluate cell viability. In untreated roots there were few cells with green fluorescence or red spots corresponding to necrotic nuclei; PI only labelled the cell walls of living cells (Fig. 6A). This indicated low stress and that the viability was not compromised. To check proper loading of H_2DCFDA, root segments were damaged mechanically with forceps. As a result of such manipulation, a strong green fluorescent signal could be observed (data not shown). This fact demonstrates that mechanical stress also produces oxidative damage, and emphasizes that careful manipulation is important in the preparation of the material used when minute alterations caused by heavy metals are analysed.

A different staining pattern was observed between plants grown in the presence of 30 μM Cd or Hg (Fig. 6E, G). Cd induced oxidative stress, as several epidermal cells glowed in green fluorescence of H_2DCFDA (Fig. 6E, grey arrows) and some nuclei were highlighted in red by PI (Fig. 6E, black arrows). However, in epidermal cells of Hg-treated seedlings only red condensed nuclei were observed (Fig. 6G, grey arrow). In parallel, root hair architecture was affected by both metals, as could be observed with differential interference contrast (DIC) optics (Fig. 6F, H). By contrast to healthy control root hairs (Fig. 6B), incipient plasmolysis and loss of root hair cytosolic content was also observed.

Because growth inhibition analysis showed that phytotoxic effects of both metals could be visualized earlier than 24 h (Fig. 2), the different patterns of toxicity with Cd and Hg were assessed in samples subjected to increasing doses of each metal at 6 and 24 h of exposure (Table 2). In general, symptoms of stress were clearly visible after only 6 h of exposure, and few differences in peroxidation and cell death staining could be observed with seedlings exposed for a prolonged period. Even at the lowest metal concentration, there were clear differences compared with control seedlings; when grown in 3 μM Cd, few cells showed green labelling, and even fewer were dead. At increasing concentrations, the numbers of stained cells with both H_2DCFDA and PI also increased, meaning that at higher Cd concentrations more cells were stressed and dead. Hg had apparently a stronger toxic effect, since after growing the plants in 3 μM Hg for 6 and 24 h there was a high percentage of epidermal cells stressed and already dead, similar to the data on seedlings exposed to 30 μM Cd (Table 2). Surprisingly, on exposure to Hg over 10 μM the percentage of stressed cells was similar to the control, but an extremely high proportion of dead cells appeared. Therefore, cell viability was acutely diminished after exposure to Hg. In addition, a greenish blur highlighted the inner layers of the root (data not shown), indicating that cells of the cortex and vascular tissues were experiencing oxidative stress, an effect not observed when Cd was supplied.

The addition of 1 mM BSO to the growing medium was expected to increase green fluorescence due to a starvation of GSH/hGSH, one of the main oxidative stress counteracting metabolites (May and Leaver, 1993). Indeed, BSO leads to a remarkable increase in H_2DCFDA fluorescence, mainly located around the nucleus and at the plasmalemma (Fig. 6C, grey arrow), indicating some degree of oxidative stress (Table 2). As expected, this treatment caused a severe reduction of GSH/hGSH, as measured by HPLC (over 50% of the control; data not shown). However, this

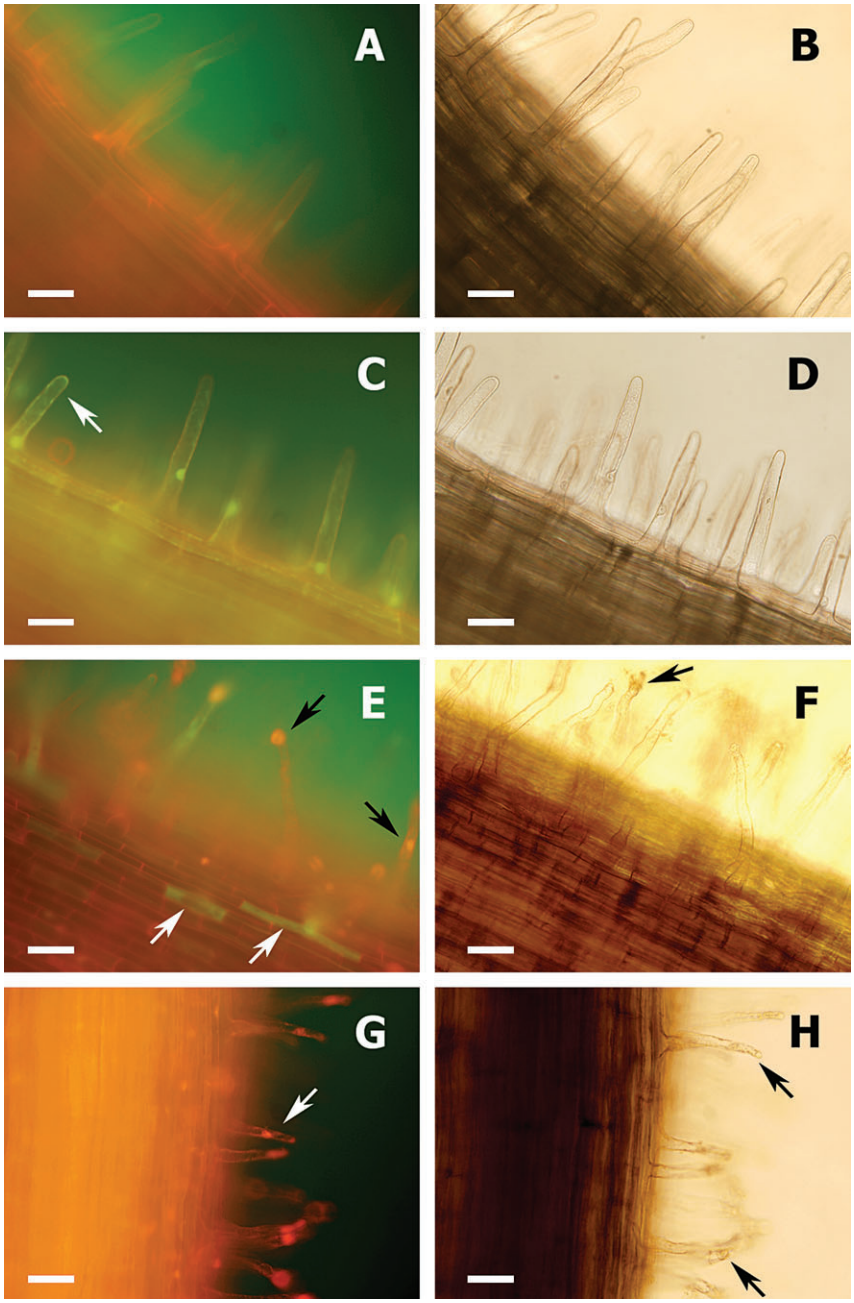

Fig. 6. H_2DCFDA and IP staining of root cells from *M. sativa* seedlings exposed for 24 h to several chemicals. Panels on the left side, dual staining with H_2DCFDA (green) and IP (red). Panels on the right side, DIC equivalent imaging of root epidermal hairs. (A, B), control; (C, D), 1 mM BSO; (E, F), 30 μM Cd; (G, H), 30 μM Hg. Arrows highlight prominent damage caused by the different chemicals used. Scale bar equals 80 μm.

treatment did not increase cell death (Table 2), nor did it affect the architecture of root hairs, as revealed through visualization by DIC optics (Fig. 6D), suggesting that cell viability was not completely compromised upon treatment with BSO.

Discussion

The kinetics of Cd and Hg toxicity, which caused among other symptoms oxidative stress, has been evaluated and compared in alfalfa plantlets. Tracing the kinetics of plant responses on short-term exposure to both metals would help to identify the mechanisms underlying toxicity. First, conventional methods were used to measure oxidative stress indexes, such as lipid peroxidation or protein oxidation. Data showed consistent responses in long-term treatments with Cd and Hg, as shown in the beaker-size hydroponic system (Fig. 1). However, the sharp inhibition in root growth and lipid peroxidation observed after 24 h in Hg-treated plants indicated that it is possible that an early

Table 2. *Cell viability (%) in* Medicago sativa *seedlings exposed to several concentrations of Cd and Hg, and to 1 mM BSO, after 6 h and 24 h*

Cells were characterized as not affected (without H_2DCFDA fluorescence), oxidative stressed cells labelled with H_2DCFDA, and dead (stained with IP and showing condensed nuclei). Over 10 different slides were quantified from at least five independent experiments. Different superscript letters denote significant differences between treatments at $P < 0.05$.

Cell viability	Control	1 mM BSO	Cd (μM)			Hg (μM)		
			3	10	30	3	10	30
6 h								
Not affected	$87^{a}\pm8$	$23^{d}\pm10$	$60^{b}\pm15$	$49^{c}\pm9$	$21^{d}\pm4$	$42^{e}\pm7$	$25^{d}\pm3$	$9^{e}\pm4$
Stressed	$8^{a}\pm5$	$73^{d}\pm14$	$31^{b}\pm16$	$39^{b}\pm7$	$57^{c}\pm4$	$32^{b}\pm18$	$15^{a}\pm15$	$9^{a}\pm5$
Dead	$4^{a}\pm4$	$6^{a}\pm2$	$9^{a}\pm5$	$12^{ab}\pm6$	$22^{b}\pm4$	$26^{b}\pm7$	$61^{e}\pm6$	$82^{d}\pm6$
24 h								
Not affected	$89^{a}\pm6$	$40^{ed}\pm22$	$77^{b}\pm13$	$59^{c}\pm12$	$42^{cd}\pm19$	$47^{cd}\pm14$	$32^{d}\pm24$	$11^{e}\pm10$
Stressed	$10^{a}\pm6$	$60^{c}\pm22$	$15^{a}\pm8$	$29^{b}\pm13$	$27^{b}\pm21$	$25^{b}\pm20$	$7^{a}\pm13$	$7^{a}\pm12$
Dead	$<1^{a}\pm1$	$<1^{a}\pm1$	$8^{ab}\pm8$	$12^{b}\pm12$	$31^{c}\pm25$	$28^{bc}\pm16$	$62^{d}\pm21$	$81^{d}\pm15$

linear response had been missed. Thus, the microscopic assay was used to shorten exposure to metal. In these experiments, growth inhibition (Fig. 2) and qualitative and quantitative non-protein thiol content variations (Fig. 3; Table 1) revealed that plants were undergoing important physiological changes upon exposure to Cd and Hg. In particular, growth was inhibited very early, in agreement with data from other authors on *Pinus sylvestris* and poplar seedling roots supplied with 50 μM Cd (Schützendübel *et al*., 2001, 2002).

On the other hand, no clear symptoms of oxidative stress could be detected by the conventional techniques used to trace oxidative stress. It seemed, therefore, that a more adequate methodology was necessary to trace rapid toxic effects. With this aim epifluorescence analysis was employed, novel fluorescent probes being used to monitor oxidative stress at the cellular level. Thus, the accumulation of peroxides as a result of adding heavy metal was demonstrated by H_2DCFDA (Fig. 6E, G). It has permitted the different ability of each metal to trigger various stress responses in alfalfa seedlings, exposed for 6 and 24 h, to be assessed. Comparing the toxic effects of each treatment at both sampling periods, no significant differences in cellular damage were observed, which might indicate that after 6 h a remarkable degree of oxidative damage had already been reached (Table 2). In a similar experimental design, accumulation of H_2O_2 was followed in Scots pine seedling roots using a histochemical staining that increased with time (Schützendübel *et al*., 2001), but detailed cellular analysis could not be achieved. Counterstaining with IP also revealed that cell death augmented concomitantly to Cd concentration (Table 2; Fig. 6E). Paradoxically, Hg did not trigger a clear increase in lipid peroxidation in epidermal cells (Fig. 6G). However, cell viability was drastically reduced with rising concentrations of this metal, since cell death reached high values (80%; Table 2). All these results were supported by the increase in the IP:MCB ratio in the experiments carried out to visualize changes in the GSH/hGSH cellular pool by confocal microscopy (Fig. 4). Finally, the inner root cells (i.e. cortex and/or endodermis) of plants grown for 24 h in 30 μM Hg had a greenish glow (data not shown), an effect that was not observed at 6 h of exposure nor in plants treated with Cd. This might imply that those cells were undergoing oxidative stress, probably as cellular damage expanded to more internal layers of cells in roots under Hg exposure. Taking all the data together, the present results suggest that Hg produced a quicker and stronger toxicity than Cd, as already suggested by the long-term exposure in the beaker-size experiments. It is conceivable that dead cells were metabolically non-functional and had lost the capability to metabolize H_2DCFDA, being therefore unable to show up fluorescence. Consequently, no green fluorescence could be recorded at the epidermis. Similar conclusions could be drawn after observing visible root hairs; Cd-treated plants showed slight cell damage (Fig. 6F), whereas effects apparently more acute and frequent were found in seedlings grown with Hg (Fig. 6H) that suffered clear plasmolysis and loss of cytosolic content. Fojtová and Kovaric (2000) found similar cellular damage in tobacco BY2 cells cultured in the presence of 50 μM Cd, where dense and shrunken protoplasts were visualized after a 5 d treatment.

The accumulation of PCs in response to Cd and Hg was relatively low after 24 h of treatment (Fig. 3; Table 1) compared with the cellular damage found; only Cd caused the accumulation of a detectable amount of PCs. Another significant change in non-protein thiol concentration was the reduction in hGSH observed under 30 μM Hg for 24 h (Table 1). Overall, these results were in agreement with those reported for tobacco (Vögeli-Lange and Wagner, 1996), *Arabidopsis* (Xiang and Oliver, 1998), and pine (Schützendübel *et al*. 2001) after short-term treatments with Cd. In these three cases, there were minor reductions of GSH tissue content followed by increases at prolonged exposure times. Indeed, a similar trend has also been observed in alfalfa and maize plants grown in the beaker-size hydroponic system for different exposure times (data not shown). On the other hand, Hg is a poorer PC synthesis

inductor compared with Cd, both analysed *in vitro*, with recombinant phytochelatin synthase (Ha *et al*., 1999), or *in vivo* in *Rubia tinctorum* root cell cultures (Maitani *et al*., 1996). Increasing evidence supports the idea of PCs been involved only partially in metal detoxification, a mechanism probably highly dependent on the metal supplied and the plant species assessed (Landberg and Greger, 2004), as found in the hyperaccumulator *Thlaspi caerulescens* and other metallophytes (Ebbs *et al*., 2002; Schat *et al*., 2002). Additionally, transgenic *Arabidopsis thaliana* overexpressing recombinant phytochelatin synthase was more sensitive to Cd (Lee *et al*., 2003). Therefore, it is conceivable that PCs are not the first mechanism involved in heavy metal tolerance. However, they might probably work along with other mechanisms in plants subjected to longer treatments with metals (Cobbett and Goldsbrough, 2002).

GSH and hGSH are regarded as important metabolites that contribute to the control of cell redox homeostasis (May *et al*., 1998). It has been possible to monitor changes in GSH/hGSH levels in alfalfa root cells after staining with MCB, and an extensive quenching has been found associated with the supply of Cd and Hg (Fig. 4). The present results are in agreement with those reported on *A. thaliana* cells grown in medium containing Cd (10–1000 μM) and Hg (1–100 μM) by Meyer and Fricker (2002), which caused a severe MCB fluorescence depletion. This could be due to direct interaction of the metals with the nucleophyllic SH^- of GSH/hGSH, since there was an obliteration of the fluorescence emitted by the GSH–MCB adduct in the presence of both metals *in vitro* (Fig. 5). The production of the GSH/hGSH–MCB adduct *in vivo* is mediated by GST (Gutierrez-Alcalá *et al*., 2000; Hartmann *et al*., 2003), and an inhibition of the enzyme induced by heavy metals might also account for the loss of fluorescence observed. However, the present data on GST activity *in vitro* of seedlings exposed to Cd and Hg indicate that the enzyme was not affected by the heavy metals; therefore, GST seems not to be limiting in the formation of the GSH/hGSH–MCB adduct. The present observations are also in agreement with the reported affinity of those metals to bind to GSH, forming metal-thiolate compounds (Mehra *et al*., 1996; Morelli *et al*., 2002). In particular, it is considered that this might be the case in Cd-treated seedlings, which experienced few changes in GSH and hGSH tissue contents (Table 1). However, in Hg-treated seedlings the quenching of MCB fluorescence might be partially attributed to the significant depletion observed in hGSH (Table 1). Therefore, upon exposure to Cd or Hg, the thiol residue of GSH might be blocked by the formation of metal-thiolate bonds or by its oxidation to GSSG, which would diminish the reductant capability of the GSH/hGSH cellular pool. On the other hand, the putative competition of Cd or Hg with MCB to bind GSH/hGSH would make it difficult to ascertain the fate (complexation and/or oxidation) of these thiols under heavy metal stress by direct observation using confocal microscopy. Indeed, the dynamic response of MCB staining was less clear than that of H_2DCFDA, since little difference in fluorescence was observed between seedlings kept for 6 h at several levels of metals in the growing solution (Fig. 4E).

As stated before, GSH and hGSH are important antioxidants (May *et al*., 1998), which are necessary for coping with several environmental stresses. Depletion of GSH/hGSH, as observed under treatment with 1 mM BSO (Fig. 4B), led to the appearance of oxidative stress in alfalfa seedling roots to a high extent (Fig. 6C; Table 2), in agreement with May and Leaver (1993). Interestingly, no cell death was found, indicating that cells were still capable of surviving in such conditions. However, under metal stress, both cell death and oxidative stress appeared, depending on the degree of toxicity (Fig. 6; Table 2). This finding might imply that, with Cd or Hg, alteration of the GSH/hGSH pool is not the only explanation of the induction of metal toxicity, and other mechanisms of phytotoxicity might be involved. In this respect, it is known that plants subjected to environmental stresses augment their capability to draw back ROS (May and Leaver, 1993), so that they can survive, but irreversible damage and cell death occurs when that capability is overridden.

Summing up, a promising new and sensitive technique that allows detection of minute changes in oxidative damage, which might be useful to characterize cellular responses to heavy metals, has been used. Subtle differences between Cd and Hg could be observed, indicating different mechanisms of toxicity that eventually compromise cell viability. Alterations in the GSH/hGSH cellular pool in plants under heavy metal treatment could also be detected. However, it was not possible to tell whether this lower fluorescence level was due to a real GSH/hGSH pool depletion or to a metal–thiolate complex formation. Work is in progress to characterize in detail the putative metal–thiolate interaction and the amount of heavy metals taken up by discrete root cells.

Acknowledgements

The authors gratefully acknowledge the financial support of the Spanish Ministry of Education and Science (REN2002-04229-C02-01) and of Fundación Ramón Areces, which made possible this work, specially the PhD grant received by COV from Fundación Ramón Areces. We also thank the comments of two anonymous reviewers which allowed substantial improvement of the manuscript.

References

Allan AC, Fluhr R. 1997. Two distinct sources of elicited reactive oxygen species in tobacco epidermal cells. *The Plant Cell* **9,** 1559–1572.

Bethke PC, Jones RL. 2001. Cell death of barley aleurone protoplasts is mediated by reactive oxygen species. *The Plant Journal* **25,** 19–29.

Cho U-H, Park J-O. 2000. Mercury-induced oxidative stress in tomato seedlings. *Plant Science* **156,** 1–9.

Cobbett C, Goldsbrough P. 2002. Phytochelatins and metallothioneins: roles in heavy metal detoxification and homeostasis. *Annual Review of Plant Biology* **53,** 159–182.

Dalton DA, Joyner SL, Becana M, Iturbe-Ormaetxe I, Chatfield JM. 1998. Antioxidant defenses in the peripheral cell layers of legume root nodules. *Plant Physiology* **116,** 37–43.

Dixit V, Pandey V, Shyam R. 2001. Differential antioxidative responses to cadmium in roots and leaves of pea (*Pisum sativum* L. cv. Azad). *Journal of Experimental Botany* **52,** 1101–1109.

Ebbs S, Lau I, Ahner B, Kochian L. 2002. Phytochelatin synthesis is not responsible for Cd tolerance in the Zn/hyperaccumulator *Thlaspi caerulescens* (J. & C. Presl). *Planta* **214,** 635–640.

Fojtová M, Kovařík A. 2000. Genotoxic effect of cadmium is associated with apoptotic changes in tobacco cells. *Plant, Cell and Environment* **23,** 531–537.

Fricker MD, Meyer AJ. 2001. Confocal imaging of metabolism *in vivo*: pitfalls and possibilities. *Journal of Experimental Botany* **52,** 631–640.

Gutiérrez-Alcalá G, Gotor C, Meyer AJ, Fricker M, Vega JM, Romero LC. 2000. Glutathione biosynthesis in *Arabidopsis* trichome cells. *Proceedings of the National Academy of Sciences, USA* **97,** 11108–11113.

Ha S-B, Smith AP, Howden R, Dietrich WM, Bugg S, O'Connell MJ, Goldsbrough PB, Cobbett CS. 1999. Phytochelatin synthase genes from *Arabidopsis* and the yeast *Schizosaccharomyces pombe*. *The Plant Cell* **11,** 1153–1163.

Hall JL. 2000. Cellular mechanisms for heavy metal detoxification and tolerance. *Journal of Experimental Botany* **53,** 1–11.

Hartmann TN, Fricker MD, Rennenberg H, Meyer AJ. 2003. Cell-specific measurement of cytosolic glutathione in poplar leaves. *Plant, Cell and Environment* **26,** 965–975.

Heidstra R, Geurts R, Franseen H, Spaink HP, Van Kammen A, Bisseling T. 1994. Root hair deformation activity of nodulation factors and their fate on *Vicia sativa*. *Plant Physiology* **105,** 787–797.

Howden R, Goldsbrough PB, Andersen CR, Cobbett CS. 1995. Cadmium-sensitive, *cad1* mutants of *Arabidopsis thaliana* are phytochelatin deficient. *Plant Physiology* **107,** 1059–1066.

Landberg T, Greger M. 2004. No phytochelatin (PC2 and PC3) detected in *Salix viminalis*. *Physiologia Plantarum* **121,** 481–487.

Lee S, Moon JS, Ko T-S, Petros D, Goldsbrough PB, Korban SS. 2003. Overexpression of *Arabidopsis* phytochelatin synthase paradoxically leads to hypersensitivity to cadmium stress. *Plant Physiology* **131,** 656–663.

Lozano-Rodriguez E, Hernández LE, Bonay P, Carpena-Ruiz RO. 1997. Distribution of cadmium in shoot and root tissues of maize and pea plants: physiological disturbances. *Journal of Experimental Botany* **306,** 123–128.

Maitani T, Kubota H, Sato K, Yamada T. 1996. The composition of metals bound to class III metallothionein (phytochelatin and its desglycyl peptide) induced by various metals in root cultures of *Rubia tinctorum*. *Plant Physiology* **110,** 1145–1150

Matamoros MA, Moran JF, Iturbe-Ormaetxe I, Rubio MC, Becana M. 1999. Glutathione and homoglutathione synthesis in legume root nodules. *Plant Physiology* **121,** 879–888.

May MJ, Leaver CJ. 1993. Oxidative stimulation of glutathione synthesis in *Arabidopsis thaliana* suspension cultures. *Plant Physiology* **103,** 621–627.

May MJ, Vernoux T, Leaver C, Van Montagu M, Inzé D. 1998. Glutathione homeostasis in plants: implications for environmental sensing and plant development. *Journal of Experimental Botany* **49,** 649–667.

Mehra RK, Miclat J, Kodati VR, Abdullah R, Hunter TC, Mulchandani P. 1996. Optical spectroscopic and reverse-phase HPLC analyses of Hg(II) binding to phytochelatins. *Biochemical Journal* **314,** 73–82.

Meuwly P, Rauser WE. 1992. Alteration of thiol pools in roots and shoots of maize seedlings exposed to cadmium-adaptation and developmental cost. *Plant Physiology* **99,** 8–15.

Meuwly P, Thibaul P, Schwan AL, Rauser WE. 1995. Three families of thiol peptides are induced by cadmium in maize. *The Plant Journal* **7,** 391–400.

Meyer AJ, Fricker MD. 2002. Control of demand-driven biosynthesis of glutathione in green *Arabidopsis* suspension culture cells. *Plant Physiology* **130,** 1927–1937.

Meyer AJ, May MJ, Fricker M. 2001. Quantitative *in vivo* measurement of glutathione in *Arabidopsis* cells. *The Plant Journal* **27,** 67–78.

Morelli E, Cruz BH, Somovigo S, Scarano G. 2002. Speciation of cadmium-γ-glutamyl peptides complexes in cells of the marine microalga *Phaeodactylum tricornutum*. *Plant Science* **163,** 807–813.

Noctor G, Arisi ACM, Jouanin L, Kunert KJ, Rennenberg H, Foyer CH. 1998. Glutathione: biosynthesis, metabolism and relationship to stress tolerance explored in transformed plants. *Journal of Experimental Botany* **49,** 623–647.

Noctor G, Gómez L, Vanacker H, Foyer CH. 2002. Interactions between biosynthesis, compartmentation and transport in the control of glutathione homeostasis and signalling. *Journal of Experimental Botany* **53,** 1283–1304.

Potikha TS, Collins CC, Johnson DI, Delmer DP, Levine A. 1999. The involvement of hydrogen peroxide in the differentiation of secondary walls in cotton fibers. *Plant Physiology* **119,** 849–858.

Rauser WE. 1991. Cadmium-binding peptides from plants. *Methods in Enzymology* **205,** 319–333.

Rauser WE. 1995. Phytochelatins and related peptides: structure, biosynthesis, and function. *Plant Physiology* **109,** 1141–1149.

Romero-Puertas MC, Palma JM, Gómez M, Del Río LA, Sandalio LM. 2002. Cadmium causes the oxidative modification of proteins in pea plants. *Plant, Cell and Environment* **25,** 677–686.

Salt DE, Blaylock M, Kumar NPBA, Dushenkov V, Ensley BD, Chet I, Raskin I. 1995 Phytoremediation: a novel strategy for the removal of toxic metals from the environment using plants. *Biotechnology* **13,** 468–474.

Sánchez-Fernández R, Fricker M, Corben LB, White NS, Sheard N, Leaver CJ, Van Montagu M, Inzé D, May MJ. 1997. Cell proliferation and hair tip growth in the *Arabidopsis* root are under mechanistically different forms of redox control. *Proceedings of the National Academy of Sciences, USA* **94,** 2745–2750.

Sandalio LM, Dalurzo HC, Gomez M, Romero-Puertas MC, Del Río LA. 2001. Cadmium-induced changes in the growth and oxidative metabolism of pea plants. *Journal of Experimental Botany* **52,** 2115–2126.

Schat H, Llugany M, Vooijs R, Hatley-Whitaker J, Bleeker PM. 2002. The role of phytochelatins in constitutive and adaptive heavy metal tolerances in hyperaccumulator and non-hyperaccumulator metallophytes. *Journal of Experimental Botany* **53,** 2381–2392.

Schüzendübel A, Nikolova P, Rudolf C, Polle A. 2002. Cadmium- and H_2O_2-induced oxidative stress in *Populus*×*canescens* roots. *Plant Physiology and Biochemistry* **40,** 577–584.

Schützendübel A, Polle A. 2002. Plant responses to abiotic stresses: heavy metal-induced oxidative stress and protection by mycorrhization. *Journal of Experimental Botany* **53,** 1351–1365.

Schützendübel A, Schwanz P, Teichmann T, Gross K, Langenfeld-Heyser R, Goldbold DL, Polle A. 2001. Cadmium-induced

changes in antioxidative systems, hydrogen peroxide content, and differentiation in Scots pine roots. *Plant Physiology* **127,** 887–898.

Skipsey M, Andrews CJ, Townson JK, Jepson I, Edwards R. 1997. Substrate and thiol specificity of a stress-inducible glutathione transferase from soybean. *FEBS Letters* **409,** 370–374.

Vögeli-Lange R, Wagner GW. 1996. Relationship between cadmium-, glutathione- and cadmium-binding peptides (phytochelatins) in leaves of intact tobacco seedlings. *Plant Science* **114,** 11–18.

Xiang C, Oliver DJ. 1998. Glutathione metabolic genes co-ordinately respond to heavy metals and jasmonic acid in *Arabidopsis*. *The Plant Cell* **10,** 1539–1550.